analytical chemistry

ARTICLE

pubs.acs.org/ac

Tunnel Frit: A Nonmetallic In-Capillary Frit for Nanoflow Ultra High-Performance Liquid Chromatography−Mass SpectrometryApplications

Chao-Jung Chen,[†,‡] Wei-Yun Chen,[§] Mei-Chun Tseng,[∥] and Yet-Ran Chen[*,§]

[†]Proteomics Core Laboratory, Department of Medical Research, China Medical University Hospital, Taichung 404, Taiwan

[‡]Graduate Institute of Integrated Medicine, China Medical University, Taichung 404, Taiwan

[§]Agricultural Biotechnology Research Center and [∥]Institute of Chemistry, Academia Sinica, Taipei, Taiwan 11529

Supporting Information

ABSTRACT: In this study, an easy method to fabricate a durable in-capillary frit was developed for use in nanoflow liquid chromatography (nanoLC). A small orifice was tunneled into the sol−gel frit during the polymerization process resulting in the simple fabrication of a tunnel frit. A short packing tunnel frit column (2 cm, C_{18} particles) was able to sustain over 10 000 psi continuous liquid flow for 10 days without observation of particle loss, and back pressure variation was less than 5%. The tunnel frit was successfully applied to the fabrication of nanoflow ultra high-performance liquid chromatography (nano-UHPLC) trap and analytical columns. In the analysis of tryptic peptides, the tunnel frit trap and analytical columns were demonstrated to have high separation efficiency and sensitivity. In analysis of phosphopeptides, the use of the nonmetallic tunnel frit column showed better sensitivity than the metallic frit column. This design can facilitate the preparation of nano-HPLC and nano-UHPLC columns and the packing material can easily be refilled when the column is severely contaminated or clogged.

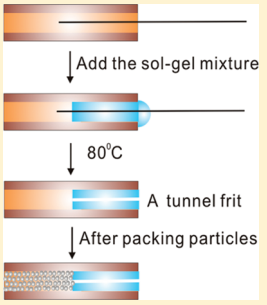

The complexity and broad dynamic range of the proteome presents great analytical challenges in global proteomic profiling. Because of its high-sensitivity, high resolving power, and the robustness of the instrumentation for polypeptide analysis, the nano-HPLC−MS system has developed into the major analytical platform for proteomics research.[1−4] Chromatographic performance is considered to be the critical factor for the success of qualification and quantitation in proteomics using nano-HPLC−MS. However, the reproducibility and lifetime of the nano-HPLC columns is rather limited in comparison with the conventional HPLC columns. The nano-HPLC columns can be easily damaged by the small particles (such as polyacrylamide gel residues) or hydrophobic molecules (such as detergents or undigested proteins).[5,6] In the fabrication of new nano-HPLC capillary columns to replace damaged ones, the method used to retain the packing particles is still a key technology. Currently, most nano-HPLC columns are made by packing particles into a tapered tip or frit capillary. To prepare a tapered tip capillary, one end of the column is heat-drawn to create a small aperture (10−20 μm), thus creating a "keystone" effect to retain the packing material; the tapered tip of the column also acts as an emitter of electrospray ionization (ESI).[7−11] The fabrication of the tapered tip capillary is simple and has minimized postcolumn dead volume, which reduces band broadening due to longitudinal diffusion. However, if the tip is cracked or contaminated, the whole column has to be discarded and replaced with a new one to maintain the ionization efficiency. Because of the reduced outer diameter at the tapered end, the tapered tip capillary cannot be used for the fabrication of trap columns.

Currently, most trap columns in nano-HPLC systems are made from frit capillaries. The frit capillary is not only used in the fabrication of trap columns, it is also commonly used for the fabrication of analytical columns. For the application of frit analytical columns to nano-HPLC−MS, an ESI emitter is connected to the outlet of the analytical column with a zero dead volume (ZDV) union. With this design, the ESI emitter or analytical column can be replaced independently when the ionization or separation efficiency decreases. However, fabrication of in-capillary frits is challenging because the frit should not only have enough strength to support the packing material but also have high permeability for liquid flow. Several methods are used for fabrication of in-capillary frits. For example, the frit can be fabricated by sintering glass beads inside the capillary.[12−14] However, using this method, it is hard to optimize the fast sintering reaction, usually resulting in production of frit columns that have inconstant liquid permeability and pressure tolerance. In addition, the sintering process can result in the loss of the polyimide layer at the capillary end, which can cause the column end to be fragile to mechanical stress.[15] Sol−gel frit capillaries can be fabricated without sintering and thus preserve the polyimide coating and be more tolerant to the mechanical stress;[16] however, the liquid permeability of sol−gel frits is not reproducible and may produce significantly high back pressure during liquid flow.[17] To further improve the liquid permeability and

Received: September 26, 2011
Accepted: November 18, 2011
Published: November 18, 2011

fabrication reproducibility of the sol−gel based frit, a modified method mixing sol−gel with silica gel particles or glass fiber disk has been developed.[17] However, pressure tolerance higher than 3 000 psi has not yet been demonstrated.

To further enhance nano-HPLC−MS performance, a recent development in ultra high-performance liquid chromatography (UHPLC) systems has been successfully applied to nanoflow LC−MS systems.[18,19] Nano-UHPLC normally utilizes 1.7 μm C_{18} particles in the analytical column, thus creating significantly higher back pressure in comparison with the conventional nano-HPLC (5 μm particles) during peptide separation. This design enhances the separation resolution and thus facilitates the sensitivity of analysis of complicated peptide mixtures.[18] These enhancements have been demonstrated to be of benefit to both protein identification and quantitation performance.[20,21]

However, there are still several challenges concerned with connecting capillary columns to the nano-UHPLC system. In nano-UHPLC−MS, the system back pressure can be as high as 9 000 psi, thus the connection fittings should be able to tolerate >10 000 psi. It is also important that the frit is able to sustain high liquid pressure. This is particularly important in trap column frits because the short lengths of packing (~2 cm) and the high flow-rate applied to the trap column can result in relatively higher pressure on the frit in comparison with the analytical column. The use of a stainless steel frit can help the trap column to sustain high pressure. However, the use of stainless steel may cause absorption of phosphate groups, which results in a lower recovery of phosphopeptides.[22,23] In addition, this design also has larger dead volume between the trap and the analytical column, which can reduce separation efficiency. Moreover, for the analytical column, it is more difficult to use a tapered tip capillary in preparation of a nano-UHPLC column. This is because a smaller orifice (<10 μm) is required to retain smaller particles and maintain ESI stability. The use of the smaller orifice tapered tip column can prolong the packing time and make the tip more fragile.

Thus, to fabricate a nonmetallic in-capillary frit for both nano-HPLC and nano-UHPLC applications, it is important that the frit has several characteristics. First, because of the use of UHPLC fittings, the polyimide coating on the capillary column ends must be preserved to avoid column crushing due to the high tightening strength of the UHPLC fittings. Second, the pressure tolerance of the packed frit capillary column should be higher than 10 000 psi. Third, the frit should have high liquid permeability and not get clogged by the packing particles even when small packing particles are used.

In this study, a simple method for the preparation of a high mechanical strength and low back pressure tunnel frit was developed. The tunnel frit was applied to both trap and analytical nano-UHPLC columns. Application of this design not only enhanced the nano-UHPLC separation resolution but also improved the sensitivity of the phosphopeptide analysis.

EXPERIMENTAL SECTION

Materials. Tris(2-carboxyethyl) phosphine hydrochloride (TCEP), methyl methanethiosulfonate (MMTS), formamide, 4-(2-hydroxyethyl) piperazine-1-ethanesulfonic acid (HEPES), Triton X-110 (TX-100), sodium orthovanadate, sodium bicarbonate, sodium pyruvate, potassium chloride, potassium phosphate monobasic, sodium chloride, sodium phosphate dibasic, anhydrous ethylenediaminetetraacetic acid (EDTA), lactic acid, trifluoroacetic acid (TFA), and formic acid were purchased from Sigma (St. Louis, MO). Kasil 1 potassium silicate was purchased from PQ Corporation (Valley Forge, PA). Methanol (LC−MS grade), acetonitrile (ACN, LC−MS grade), sodium dodecyl sulfate (SDS), ammonium hydroxide, and urea were purchased from J. T. Baker (Phillipsburg, NJ). RPMI-1640 medium, penicillin, streptomycin, MEM NEAA, and fetal bovine serum were purchased from Invitrogen (Carlsbad, CA). Trypsin (modified, sequencing grade) was from Promega (Madison, WI). The phosphatase inhibitor cocktail was purchased from Hoffmann-La Roche (Basel, Switzerland). Tryptic enolase was purchased from Waters (Milford, MA). For LC−MS analysis, the acetonitrile (ACN) with 0.1% formic acid (FA) and water with 0.1% formic acid (LC−MS grade, J. T. Baker, Phillipsburg, NJ) were used as the mobile phase. Deionized water (18.1 MΩ cm resistivity) from Milli-Q system (Millipore, Bedford, MA) was used throughout this work.

Preparation of Tunnel Frit Packed Columns. To fabricate the tunnel frit capillary for the analytical and trap columns, 15 and 18 μm tungsten wires (Scientific Instrument Service, SIS, NJ) were used, respectively. The fabrication was performed by inserting about 5 mm of the 15 and 18 μm tungsten wires, respectively, into one end of a 75 μm i.d. × 365 μm o.d. capillary (Polymicro Technologies, Phoenix, AZ) and a 180 μm i.d. × 365 μm o.d capillary. The sol−gel solution was prepared by mixing 170 μL of Kasil 1 potassium silicate (20.8%) with 20 μL of formamide (99.5%) and vortexing for 1 min. The wire-inserted end of the capillary was dipped into a 2 μL sol−gel mixture, and the sol−gel slightly flowed into the column with the capillary action. The capillary was then incubated in an oven at 60 °C for 10 min, and the tungsten wire was removed from the capillary. After removing the tungsten wire, the capillary was incubated in an 80 °C oven overnight. When the tunnel frit was completely polymerized, the tunnel frit column was washed with methanol at a flow rate of 0.1 mL/min and then the frit quality was checked under a microscope (SZ-ST, Olympus, Tokyo, Japan) and the size was evaluated by a scanning electron microscope (ULTRA plus, Zeiss, Germany).

To pack the stationary phase particles into a tunnel frit capillary, a packing slurry was prepared by mixing 2 mg of packing materials with 1 mL of methanol. The slurry vial was sonicated for 5 min to prevent aggregation prior to packing. After sonication, both the slurry and capillary were placed in the pressure cell (Brechbuehler, Schlieren, Switzerland). The slurry was pumped into the capillary column by pressurizing the vessel to 1 000 psi using helium gas. For the trap column, a slurry of 5 μm particles (Symmetry C_{18}, Waters, Milford, MA) was packed into the capillary until the packing was 2 cm in length. For the analytical column, a slurry of 5 μm particles (Symmetry C_{18}, Waters, Milford, MA) was first packed into the capillary until the packing was 5 mm in length, then a slurry of 1.7 μm particles (BEH130 C_{18}, Waters, Milford, MA) was used until a 25 cm packing length was reached. The packed column was then removed from the pressure vessel ready for further use.

Nano-UHPLC−MS Analysis. LC−MS was performed with a nanoflow LC system (nanoACQUITY UPLC, Waters, Millford, MA) coupled with a hybrid Q-TOF mass spectrometer (Synapt HDMS, Waters, Manchester, U.K.). The sample was injected into a stainless steel frit trap column (Symmetry C_{18}, 5 μm, 180 μm × 20 mm, Waters, Milford, MA) or the tunnel frit trap column with a flow rate of 8 μL/min and a duration of 1.5 min. The trapped analytes were separated by a commercial analytical column (BEH130 C_{18}, 1.7 μm, 75 μm × 250 mm, Waters, Milford, MA) or the tunnel frit analytical column with a flow rate of 300 nL/min. An

acetonitrile/water gradient of 12−80% for 23 min and 10−90% for 80 min was used for analysis of tryptic enoloase peptides and Jurkat phosphopeptides, respectively. For MS analysis, the data dependent acquisition method was set to one full MS scan (400−1600 m/z) with 0.6 s scan time and switched to three 1.2 s product ion scans (100−1990 m/z) when a precursor ion with the charge 2+, 3+, and 4+ and the intensity greater than 20 counts was detected. Before each of the sample analyses, 50 fmol of tryptic enolase peptides was used to confirm the column efficiency and LC−MS sensitivity.

Cell Culture and Cell Stimulation. Jurkat cells, clone E6-1 were purchased from the Bioresource Collection and Research Center (BCRC60424, BCRC, Hsinchu, Taiwan). The cells were cultured in RPMI 1640 medium supplemented with 10% fetal bovine serum, 0.1 mM MEM NEAA, 50 μg/mL penicillin, 50 μg/mL streptomycin, 1 mM sodium pyruvate, 25 mM sodium bicarbonate, and 10 mM HEPES in an incubator with 5% CO_2 at 37 °C. Before cell stimulation, cells were pelleted by centrifugation (700g) for 10 min and reconstituted with RPMI 1640 medium (5×10^6 cells/mL) in a CO_2 incubator for 2 h. Cells were then stimulated with 10% fetal bovine serum and 500 μM sodium pervanadate at 37 °C for 30 min. The cells were immediately transferred into a tube with cold PBS buffer (137 mM NaCl, 2.7 mM KCl, 10 mM Na_2HPO_4, and 1.8 mM KH_2PO_4 at pH 7.5) with addition of 500 μM sodium pervanadate and 1× phosphatase inhibitor cocktail.

Cell Lysis, Protein Reduction, Alkylation, Digestion. Jurkat cells were lysed in lysis buffer (0.1% SDS, 0.02% Triton X-100, and 50 mM HEPES at pH 8.0) and subjected to three 30 min freeze−thaw cycles in a sonicator. After lysis, cell debris was pelleted and removed by centrifugation at 10 000g. The extracted protein concentration was then measured by BCA Protein Assay (Pierce, Rockford, IL). Cell lysate was diluted to 1 μg/μL with denaturing buffer (0.05% SDS, 6 M urea, 5 mM EDTA, and 50 mM HEPES at pH 8.3) and reduced with 5 mM TCEP for 1 h at 37 °C, followed by alkylation with 2 mM MMTS for 45 min at room temperature in the dark. The extracted proteins were subjected to trypsin digestion as described previously.[6]

Phosphopeptide Purification. Phosphopeptides were enriched using titanium dioxide according to a previously described protocol.[24] Briefly, a microcolumn was made by packing 3 mg of TiO_2 particles (GL Sciences, Tokyo, Japan) into a GELoader tip. Tryptic peptides were dissolved in loading buffer (300 mg/mL lactic acid in 80% ACN and 0.2% TFA) and loaded into the microcolumn. The microcolumn was washed twice with the loading buffer and then washed twice with washing buffer 1 (80% ACN with 0.2% TFA). An additional wash was performed with washing buffer 2 (50% ACN with 0.1% TFA), and the phosphopeptides were eluted with eluting buffer (0.5% NH_4OH). Eluted phosphopeptides were dried with a centrifugal concentrator ready for LC−MS/MS analysis.

Database Search. The LC−MS/MS spectra were deisotoped, centroided, and converted to a pkl file using ProteinLynx Global Server software (version 2.4; Waters, Milford, MA). The pkl files were searched against the human International Protein Index database (version 3.48) using the MASCOT search algorithm (version 2.3.0; Matrix Science, Boston, MA). The search parameters for MASCOT for peptide and MS/MS mass tolerance were ±0.1 Da and ±0.1 Da, respectively. Enzyme specificity was set as trypsin with allowance for up to two missed cleavage sites. Methionine oxidation and phosphorylation on serine, threonine, and tyrosine residuals were set as variable modifications. Peptides and phosphopeptides were considered as identified if their MASCOT individual ion score was higher than 25 ($P < 0.01$).

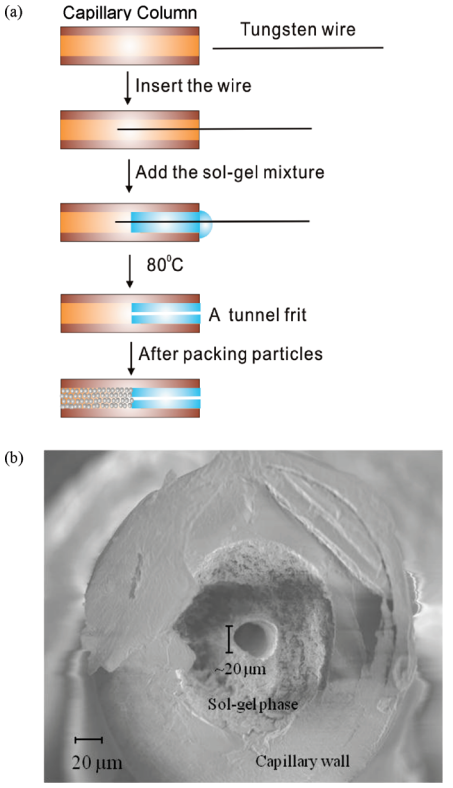

Figure 1. (a) Workflow for the preparation of a tunnel frit capillary. (b) Scanning electron microscopy scan (211× magnification) of an in-capillary tunnel frit made from a 375 μm o.d. × 180 μm i.d. capillary and 18 μm tungsten wire to produce a tunnel.

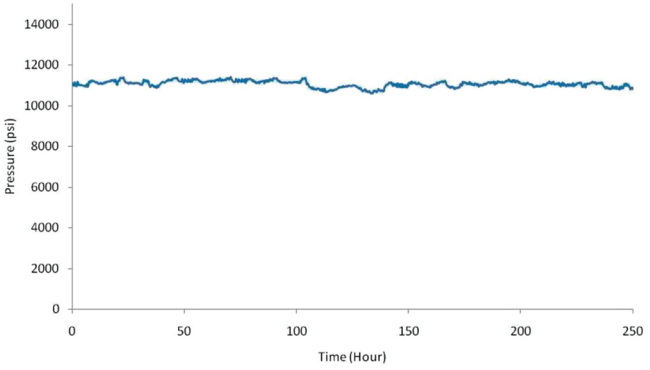

Figure 2. Long-term stability test of the tunnel frit trap column under high pressure operation with a 170 μL/min flow of H_2O/ACN = 99/1 solution.

RESULTS AND DISCUSSION

Tunnel Frit. As shown in Figure 1a, the sol−gel tunnel frit was fabricated by addition of a sol−gel mixture at the end of the column in which a tungsten wire was inserted. The use of tungsten wire is because the hardness of the tungsten metal makes it more resistant to bending during wire insertion. After sol−gel polymerization, the tungsten wire was directly removed

dx.doi.org/10.1021/ac202549y |*Anal. Chem.* 2012, 84, 297–303

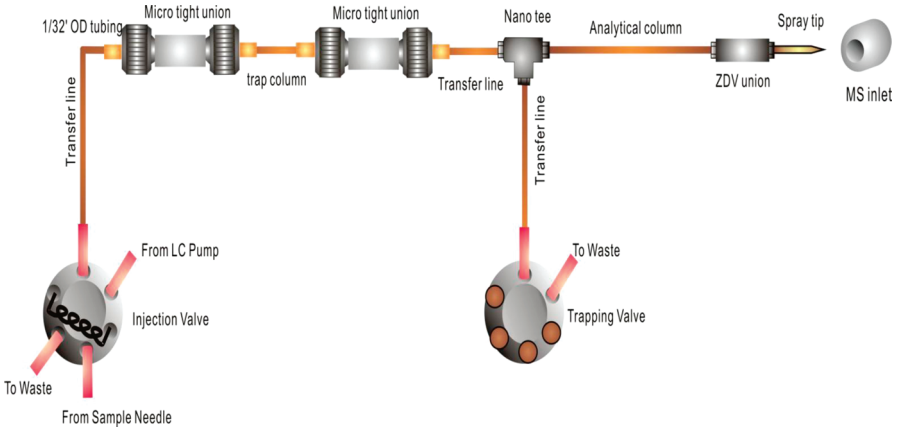

Figure 3. Schematic illustration of the application of the tunnel frit column in a nano-UHPLC−MS system.

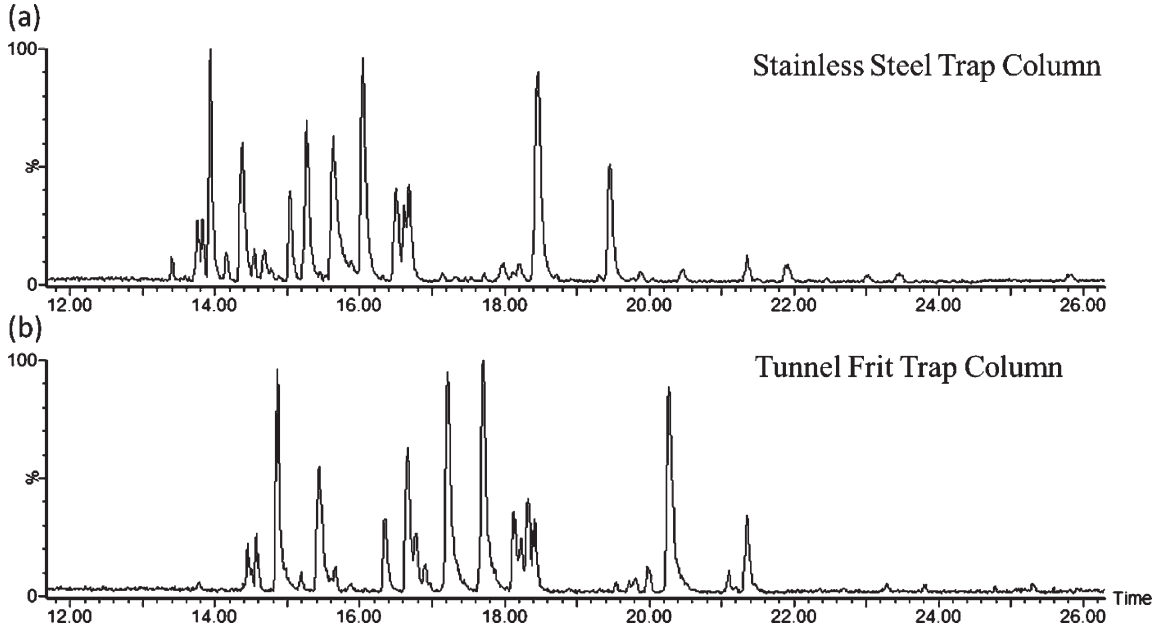

Figure 4. Base peak chromatogram for the analysis of tryptic enolase peptides (50 fmol) using nano-UHPLC−MS with (a) a stainless steel frit or (b) a tunnel frit trap column coupled with a commercial analytical column.

Table 1. Average Retention Time, Intensity and Peak Width of Selected Peptide Signals from Nano-UHPLC−MS Analyses of Tryptic Enolase Peptides (50 fmol) Replicated Six Times Using a Stainless Steel Frit or Tunnel Frit Trap Column Coupled with a Commercial Analytical Column

selected tryptic enolase peptide signal	average retention time (% RSD), min	average intensity (% RSD)	average peak fwhm (% RSD), s
	Stainless Steel Frit Trap Column		
GNPTVEVELTTEK (708.84, +2)	15.59 (0.6)	721 (5.2)	4.47 (4.0)
VNQIGTLSESIK (644.84, +2)	16.01 (0.7)	881 (3.5)	4.29 (2.0)
NVNDVIAPAFVK (643.87, +2)	18.45 (0.7)	784 (8.0)	5.01 (6.0)
TAGIQIVADDLTVTNPK (878.43, +2)	19.38 (0.3)	226 (11)	4.28 (7.6)
	Tunnel Frit Trap Column		
GNPTVEVELTTEK (708.84, +2)	17.42 (1.3)	858 (5.0)	4.32 (6.9)
VNQIGTLSESIK (644.84, +2)	17.83 (0.5)	890 (10.0)	4.35 (2.2)
NVNDVIAPAFVK (643.87, +2)	20.45 (0.8)	806 (5.2)	4.90 (1.8)
TAGIQIVADDLTVTNPK (878.43, +2)	21.55 (1.1)	308 (4.7)	4.23 (9.5)

dx.doi.org/10.1021/ac202549y |*Anal. Chem.* 2012, 84, 297–303

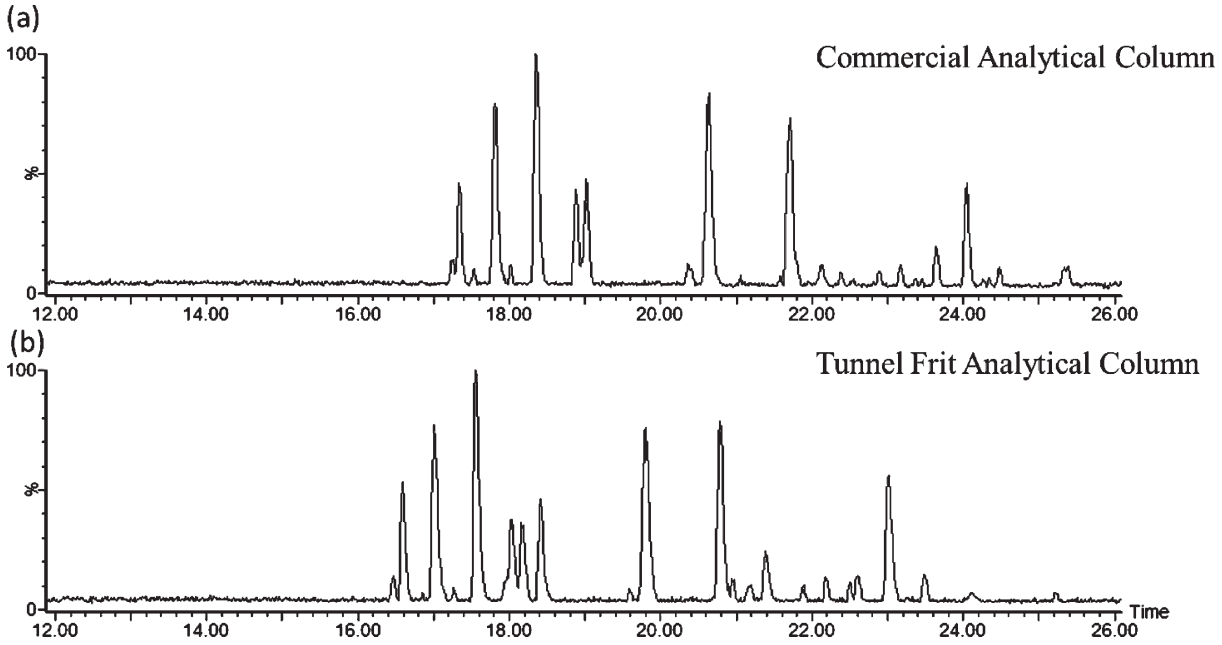

Figure 5. Base peak chromatogram for the analysis of tryptic enolase peptides (50 fmol) using nano-UHPLC−MS with a stainless steel frit trap column coupled with a (a) commercial or (b) tunnel frit analytical column.

Table 2. Average Retention Time, Intensity and Peak Width of the Selected Peptide Signals from Nano-UHPLC−MS Analyses of the Tryptic Enolase Peptides (50 fmol) Replicated Six Times Using a Stainless Steel Trap Column Coupling with a Commercial or Tunnel Frit Analytical Column

selected tryptic enolase peptide signal	average retention time (% RSD), min	average intensity (% RSD)	average peak fwhm (% RSD), s
	Commercial Analytical Column		
GNPTVEVELTTEK (708.84, +2)	17.65 (0.9)	926 (7.0)	4.8 (3.7)
VNQIGTLSESIK (644.84, +2)	18.18 (0.9)	1136 (8.7)	4.6 (3.9)
NVNDVIAPAFVK (643.87, +2)	20.54 (0.3)	888 (6.4)	5.6 (6.7)
TAGIQIVADDLTVTNPK (878.43, +2)	21.55 (0.5)	752 (6.9)	5.1 (12.3)
	Tunnel Frit Analytical Column		
GNPTVEVELTTEK (708.84, +2)	17.06 (0.4)	1018 (7.2)	5.4 (4.9)
VNQIGTLSESIK (644.84, +2)	17.51 (0.9)	1150 (9.1)	5.0 (5.9)
NVNDVIAPAFVK (643.87, +2)	19.71 (3.1)	994 (10.9)	5.7 (8.7)
TAGIQIVADDLTVTNPK (878.43, +2)	20.69 (0.1)	951 (7.3)	5.4 (6.8)

thus producing a frit with a tunnel. Because the optimal sol−gel porous structure is not required for this frit, the reproducibility of the frit is no longer controlled by the sol−gel polymerization reaction. The use of 18 μm wire to fabricate the tunnel frit in the capillary column (180 μm i.d.) resulted in a tunnel of ∼18 μm diameter in the polymerized sol−gel frit as observed using SEM imaging (Figure 1b). Excluding the final incubation time, the fabrication process for each tunnel frit column did not exceed 15 min. Several columns can therefore be prepared in parallel and incubated in the oven, making this is a simple and efficient method by which tunnel frits can be fabricated for capillary columns.

High-Pressure Tolerance of the Tunnel Frit Column. To demonstrate the high-pressure tolerance of the frit column, a short length of packing was used. A tunnel frit column packed with C_{18}, 5 μm particles (2 cm in length) was connected to the UHPLC pump, and a liquid flow of 170 μL/min (H_2O/ACN = 99/1) was applied. The trap column was able to sustain a liquid flow pressure of ∼11 000 psi for more than 10 days (maximum test time) with RSD of the pressure <1.4% (Figure 2) allowing long-term continuous flow of the solvent. No significant particle loss or pressure instability were observed during the period. This stability and long-term sustainability of high pressure illustrates that the tunnel frit column is suitable for ultra high-performance system operation. The back pressure of a 75 μm × 25 cm capillary packed with 1.7 μm particles of an analytical column is normally <9 000 psi (for the flow rate ∼300 nL/min). This is the maximum pressure difference between the inlet and outlet of the trap column which occurs when the liquid flow switches from separation mode to sample trapping mode. Moreover, the pressure limit for the nano-UHPLC pump system is normally 10 000 psi. The above test demonstrates that the tunnel frit has sufficient pressure tolerance to be applied to current nano-UHPLC systems.

dx.doi.org/10.1021/ac202549y |*Anal. Chem.* 2012, 84, 297–303

Reproducibility of the Frit Fabrication. To evaluate the reproducibility of the frit fabrication, three tunnel frit trap columns were made and tested with the same liquid flow (Figure S1 in the Supporting Information). With 24 min of continuous liquid flow, the average back pressure of the three tunnel frit trap columns was 10 116 psi with an RSD of 0.31% (column-to-column).

Setup of Tunnel Frit Trap Columns for the Nano-UHPLC System. For nano-UHPLC application, the frit column should be compatible with the ultra high-performance (UHP) fittings. As UHP fittings require high tightening strength to secure the connection of the columns, polyimide coating of the column ends is required. Because the fabrication of the tunnel frit does not involve the removal of the polyimide coating, thus the UHP fittings can be used. To make system maintenance easier, finger tight UHP fittings were used in the system (Figure 3), which makes exchanging trap and analytical columns simpler and faster.

Performance of the Tunnel Frit Trap Column. To demonstrate the feasibility of the application of the tunnel frit to trap column fabrication, the stainless steel frit column originally used in the nano-UHPLC system was replaced with the tunnel frit trap column. As shown in Figure 4, in the analysis of tryptic enolase peptides, there was no significant difference in peak intensity and peak width obtained using either the tunnel frit or the stainless frit trap columns. However, the retention time was found to be ~1 min longer when using the tunnel frit trap column in comparison with the stainless steel frit column. We attribute this mainly to the larger unpacked volume in the tunnel frit trap column resulting in the delay in the solvent gradient. To further test analytical reproducibility, six replicate analyses of tryptic enolase peptides were performed using the tunnel frit trap column in the nano-UHPLC system. The results were compared with those obtained using the stainless steel frit trap column. The RSDs of peak retention time, intensity, and fwhm (full width at half-maximum) of the tunnel frit column were smaller than 1.3%, 10%, and 9.5%, respectively, which were similar to the use of a stainless steel frit column (Table 1).

To test fabrication reproducibility, four tunnel frit trap columns were individually prepared and connected to the nano-UHPLC system. When the tryptic enolase peptides were analyzed, the RSDs of the peak retention time, intensity, and fwhm of the use of different trap columns were smaller than 1.9%, 13.0%, and 7.2%, respectively (Table S1 in the Supporting Information).

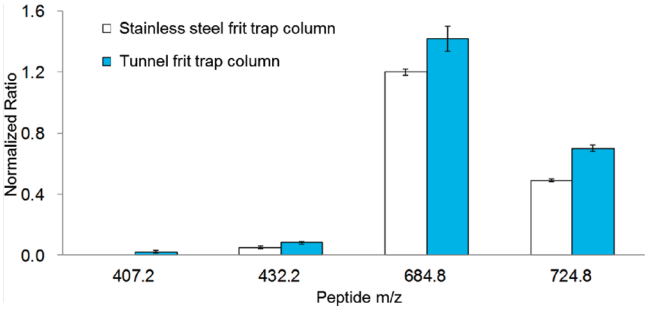

Figure 6. Normalized signal response for four synthetic phosphopeptides (NVPLYpK, m/z = 407.2, 2+; HLADLSpK, m/z = 432.2, 2+; VNQIGTpLSESIK, m/z = 684.8, 2+; and VNQIGTLSpESpIK, m/z = 724.8, 2+) analyzed using nano-UHPLC−MS with a stainless steel or tunnel frit trap column coupled with a tunnel frit analytical column. The nonphosphopeptide peptide signal (NVNDVIAPAFVK, m/z = 643.9, 2+) was used as an internal standard to normalize the phosphopeptide signal.

Application of the Tunnel Frit to the Nano-UHPLC System. In addition to the application of the tunnel frit to the trap column, the tunnel frit was also applied to the fabrication of the analytical column. In this study, 1.7 μm C_{18} particles were used as the stationary phase. With the use of a 75 μm i.d. capillary column as an analytical column, a frit with a ~15 μm diameter tunnel was used. Because the keystone effect of the ~15 μm tunnel frit was insufficient for packing 1.7 μm particles, a short section (~5 mm) of 5 μm C_{18} particles were packed first and then the 1.7 μm particles were packed until the necessary packing length was reached. As shown in Figure 5, when the same trap column (a stainless steel frit column) was used, the tunnel frit analytical column (1.7 μm, 75 μm × 250 mm) was observed to have similar separation efficiency to the commercial analytical column with the same packing material and column dimensions. The reproducibility of the analytical column was evaluated by analysis of tryptic enolase peptides. The RSDs of the peak retention time, intensity, and fwhm using the tunnel frit analytical column were smaller than 3.1%, 10.9%, and 8.7%, respectively, which were similar to those of the commercial analytical column (Table 2).

Performance of the Tunnel Frit Column System for Analysis of Phosphopeptides. Protein phosphorylation is a major protein post-translational modification that controls many important cellular signaling events.[25−27] Analyses of the dynamics of protein phosphorylation cascades help reveal significant signaling events that are correlated with the regulation of specific cellular functions. However, the dynamic nature and low abundance of phosphoproteins makes their analysis challenging.[28−33] When phosphoproteins are analyzed using nano-UHPLC−MS,

Table 3. Nano-UHPLC−MS Analysis of TiO_2 Purified Phosphopeptides from Jurkat Cell Lysate Using a Stainless Steel Frit or Tunnel Frit Trap Column Coupled with a Tunnel Frit Analytical Column

		replication 1	replication 2	replication 3	average (STD)
stainless steel frit trap column	total identified proteins	103	127	125	118 (13.3)
	ratio of phosphoproteins (%)[a]	88.3	86.6	88.0	87.6 (0.9)
	total identified peptides	190	221	210	207 (15.7)
	ratio of phosphopeptides (%)[b]	91.1	89.6	91.4	90.7 (1.0)
tunnel frit trap column	total identified proteins	158	158	171	162 (7.5)
	ratio of phosphoproteins (%)[a]	91.8	91.8	91.2	91.6 (0.3)
	total identified peptides	266	270	285	274 (10.0)
	ratio of phosphopeptides (%)[b]	92.9	92.2	92.3	92.5 (0.4)

[a] (Detected phosphoproteins/total detected proteins) × 100%. [b] (Detected phosphopeptides/total detected peptides) × 100%.

dx.doi.org/10.1021/ac202549y |Anal. Chem. 2012, 84, 297–303

the use of a metal frit may reduce the sensitivity to the phosphopeptides.[22,23] When the tunnel frit trap column was used for the analysis of four synthetic phosphopeptides and the results were compared with those obtained using a stainless steel frit trap column, the signal response with the tunnel frit trap column was about 1.2-fold (684.8 m/z, VNQIG(pT)LSESIK), 1.6-fold (432.2 m/z, HLADL(pS)K) higher than that obtained using the stainless steel frit column (Figure 6). To investigate the capability of the tunnel frit column to analyze more complicated protein mixtures, TiO_2 purified phosphopeptides from Jurket cells were analyzed by nano-UHPLC−MS using both the stainless steel frit and the tunnel frit trap column. As shown in Table 3, 162 phosphoproteins on average were observed in the tunnel frit column system, significantly more than the 118 phosphoproteins identified using the stainless steel frit system. This difference can be explained by the reduction of adsorption of phosphopeptides with the use of tunnel frit trap column.

CONCLUSIONS

In this study, a simple method for frit column fabrication using a tunnel frit was developed. The tunnel frit trap column was packed to 2 cm in length with 5 μm resins and could withstand pressure as high as 11 000 psi. In the analysis of protein digestion, the tunnel frit trap column and the tunnel frit analytical columns produced similar performance to the commercial system. To our knowledge, this is the first study that has described an in-capillary frit preparation method for nano-UHPLC applications. The successful application of our tunnel frit in nano-UHPLC−MS could substantially reduce the cost of the use of trap and analytical columns in proteomics laboratories. More importantly, this design can improve the sensitivity of analysis of phosphopeptides. The tunnel frit technique can also be widely applied to other packed columns for chromatography enrichment or separation applications.

ASSOCIATED CONTENT

Supporting Information. Additional information as noted in text. This material is available free of charge via the Internet at http://pubs.acs.org.

AUTHOR INFORMATION

Corresponding Author

*Phone: +886-2-27872050. E-mail: yetran@gate.sinica.edu.tw.

ACKNOWLEDGMENT

This work was financially supported by the Academia Sinica and the National Science Council of Taiwan. The mass spectrometry analysis was supported by the Metabolomics Core Facility, Scientific Instrument Center at Academia Sinica.

REFERENCES

(1) Winter, D.; Seidler, J.; Ziv, Y.; Shiloh, Y.; Lehmann, W. D. *J. Proteome Res.* **2009**, *8*, 418–424.
(2) Shen, Z.; Li, P.; Ni, R. J.; Ritchie, M.; Yang, C. P.; Liu, G. F.; Ma, W.; Liu, G. J.; Ma, L.; Li, S. J.; Wei, Z. G.; Wang, H. X.; Wang, B. C. *Mol. Cell. Proteomics* **2009**, *8*, 2443–2460.
(3) Qian, W. J.; Jacobs, J. M.; Liu, T.; Camp, D. G., 2nd; Smith, R. D. *Mol. Cell. Proteomics* **2006**, *5*, 1727–1744.
(4) Silva, J. C.; Gorenstein, M. V.; Li, G. Z.; Vissers, J. P.; Geromanos, S. J. *Mol. Cell. Proteomics* **2006**, *5*, 144–156.
(5) Vissers, J. P.; Chervet, J. P.; Salzmann, J. P. *J. Mass Spectrom.* **1996**, *31*, 1021–1027.
(6) Chen, C. J.; Tseng, M. C.; Lin, H. J.; Lin, T. W.; Chen, Y. R. *Anal. Chem.* **2010**, *82*, 8283–8290.
(7) Ishihama, Y.; Rappsilber, J.; Andersen, J. S.; Mann, M. *J. Chromatogr., A* **2002**, *979*, 233–239.
(8) Tan, F.; Chen, S.; Zhang, Y.; Cai, Y.; Qian, X. *Proteomics* **2010**, *10*, 1724–1727.
(9) Chen, C. J.; Chang, C. H.; Her, G. R. *J. Chromatogr., A* **2007**, *1159*, 22–27.
(10) Zheng, J.; Norton, D.; Shamsi, S. A. *Anal. Chem.* **2006**, *78*, 1323–1330.
(11) Bragg, W.; Shamsi, S. A. *J. Chromatogr., A* **2011**, *1218*, 8691–8700.
(12) Carney, R. A.; Robson, M. M.; Bartle, K. D.; Myers, P. *J. High Res. Chromatogr.* **1999**, *22*, 29–32.
(13) Cheong, W. J. *J. Chromatogr., A* **2005**, *1066*, 231–237.
(14) Rathore, A. S.; Horvath, C. *Anal. Chem.* **1998**, *70*, 3069–3077.
(15) Piraino, S. M.; Dorsey, J. G. *Anal. Chem.* **2003**, *75*, 4292–4296.
(16) Wang, L. C.; Okitsu, C. Y.; Kochounian, H.; Rodriguez, A.; Hsieh, C. L.; Zandi, E. *Proteomics* **2008**, *8*, 1758–1761.
(17) Maiolica, A.; Borsotti, D.; Rappsilber, J. *Proteomics* **2005**, *5*, 3847–3850.
(18) Eschelbach, J. W.; Jorgenson, J. W. *Anal. Chem.* **2006**, *78*, 1697–1706.
(19) Mellors, J. S.; Jorgenson, J. W. *Anal. Chem.* **2004**, *76*, 5441–5450.
(20) Miike, K.; Aoki, M.; Yamashita, R.; Takegawa, Y.; Saya, H.; Miike, T.; Yamamura, K. *Proteomics* **2010**, *10*, 2678–2691.
(21) Wang, H.; Wong, C. H.; Chin, A.; Kennedy, J.; Zhang, Q.; Hanash, S. *J. Proteome Res.* **2009**, *8*, 5412–5422.
(22) Quadroni, M. *Proteome Research: Mass Spectrometry (Principles and Practice)*; James, P., Ed.; Springer: New York, 2001; pp 189−190.
(23) Schmidt, A.; Csaszar, E.; Ammerer, G.; Mechtler, K. *Proteomics* **2008**, *8*, 4577–4592.
(24) Thingholm, T. E.; Jorgensen, T. J.; Jensen, O. N.; Larsen, M. R. *Nat. Protoc.* **2006**, *1*, 1929–1935.
(25) Di Domenico, F.; Sultana, R.; Barone, E.; Perluigi, M.; Cini, C.; Mancuso, C.; Cai, J.; Pierce, W. M.; Butterfield, D. A. *J. Proteomics* **2011**, *74*, 1091–1103.
(26) Soderblom, E. J.; Philipp, M.; Thompson, J. W.; Caron, M. G.; Moseley, M. A. *Anal. Chem.* **2011**, *83*, 3758–3764.
(27) Kosako, H.; Nagano, K. *Expert Rev. Proteomics* **2011**, *8*, 81–94.
(28) Thingholm, T. E.; Jensen, O. N.; Robinson, P. J.; Larsen, M. R. *Mol. Cell. Proteomics* **2008**, *7*, 661–671.
(29) Imanishi, S. Y.; Kochin, V.; Eriksson, J. E. *Proteomics* **2007**, *7*, 174–176.
(30) Ndassa, Y. M.; Orsi, C.; Marto, J. A.; Chen, S.; Ross, M. M. *J. Proteome Res.* **2006**, *5*, 2789–2799.
(31) Raska, C. S.; Parker, C. E.; Dominski, Z.; Marzluff, W. F.; Glish, G. L.; Pope, R. M.; Borchers, C. H. *Anal. Chem.* **2002**, *74*, 3429–3433.
(32) Iliuk, A. B.; Martin, V. A.; Alicie, B. M.; Geahlen, R. L.; Tao, W. A. *Mol. Cell. Proteomics* **2010**, *9*, 2162–2172.
(33) Iliuk, A.; Martinez, J. S.; Hall, M. C.; Tao, W. A. *Anal. Chem.* **2011**, *83*, 2767–2774.